

VIBRATION ANALYSIS OF CANDU FUEL BUNDLES DURING ON-SITE TRANSPORTATION

G.D. Morandin and T.P. Byrne

Applied Mechanics Group
Ontario Hydro, 800 Kipling Ave., Toronto, Ontario, Canada

SUMMARY

A CANDU nuclear generating station is currently evaluating the transportation of irradiated spent-fuel bundles, stored in Dry Storage Containers, from the spent fuel bays to an on-site storage facility. It is a requirement that the fuel bundles be transported in such a way that future retrieval of intact fuel will be possible. The fuel bundles are seated on trays which support the ends of the bundle at the bearing pads. Since the fuel trays and fuel bundles are subjected to vibration during transportation, an analysis is carried out in order to assess the possible fatigue damage. A finite element model of a stack of twenty-five loaded trays is subjected to an acceleration power spectra equivalent to a transport truck travelling at 20 km/h on a good-conditioned road. The results indicate that the fuel trays do not experience rms g-loads greater than 1. Hence there is no separation of fuel trays. It is shown that the stresses in the trays are below the endurance limit for 304L Stainless Steel. The largest accelerations occur at the interface between the two top trays in the stack. The acceleration trace at this location is used as input for the vibration analysis of the fuel bundle, and is applied at the three supporting bearing pads on the outer fuel pencils. The maximum stress results from the fuel bundle vibration analysis are used to predict the fatigue damage of the fuel bundle during transportation. It is shown that the fuel bundles do not experience fatigue failure when subjected to this level of vibration.

INTRODUCTION

A CANDU nuclear generating station is currently investigating the transportation of irradiated spent fuel bundles from the fuel bays to an on-site storage facility. Irradiated fuel bundles, which are stored in Dry Storage Containers (DSC), must be transported in such a way that future retrieval of intact fuel will be possible. The fuel bundles are supported on the trays by a one inch wide metal strip (Figure 1). One end of the bundle rests on a single bearing pad while the opposite end rests on two bearing pads. Each DSC contains a stack of twenty-five trays. A vibration analysis is carried out to assess damage to the fuel trays and fuel bundles during transportation.

The vibration analysis examines the motion of the fuel trays when subjected to a random ground acceleration power spectra that is representative of a transport truck travelling at 20 km/h on a good-conditioned road [Forrest 1985]. The finite element model of the 25 trays is constructed using nonlinear beam elements. Each tray is connected at the corners with compression-only analog elements (Figure 2). The weight of each fuel bundle is included as nodal loads. Only one-half of the

the fuel tray is modelled due to the geometric symmetry of the structure. The relative displacements, g-loads and stress time histories are evaluated at several locations throughout the stack. Subsequently, the maximum accelerations are applied as vibration input to the fuel bundle model. Stress component histories, at several locations in the fuel bundle, are determined and used to predict fatigue damage.

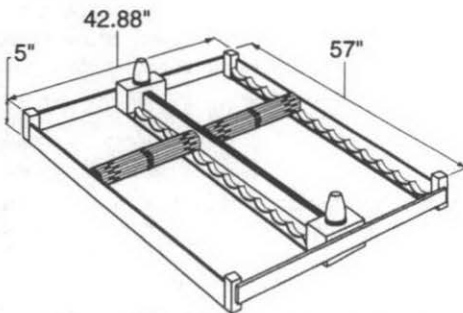


Figure 1: Irradiated Fuel Bundle Tray

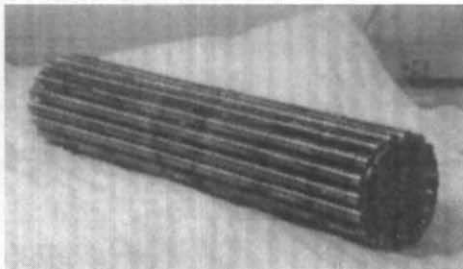


Figure 3: CANDU Fuel Bundle

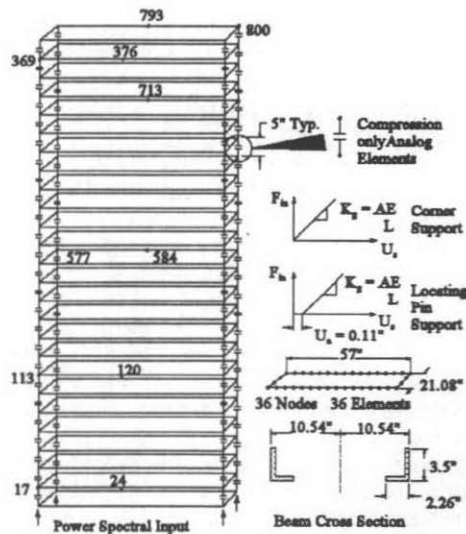


Figure 2: Spent Fuel Tray Stack Model

FUEL TRAY MODEL

The fuel tray model consists of two L-beams, which support the fuel bundles in cradles, and two cross beams connecting the L-beams (Figure 2). The fuel trays are constructed from 304L Stainless Steel and contain 24 fuel bundles aligned in two rows. Each loaded fuel tray weighs approximately 600 kg.

The DSC contains a stack of 25 trays, contacting at the corner supports and aligned with the centre locating pins. Geometric symmetry of the fuel tray permits modelling of only one-half of the tray. Each tray is modelled using 36 two-noded nonlinear beam elements available in the computer code H3DMAP [Sauvé 1995]. One L-beam of each tray is modelled with corner supports while the other L-beam is modelled with locating pin supports at the ends. Representative section properties for equivalent beams are applied to the L-beams and cross beams. In order to verify the section properties for the L-beams, the mid-span deflection from a static-analysis run is compared to the classic solution for a simply supported beam with a uniformly distributed load [Beer 1981]. The classical static deflection solution of 0.0184 inches compares well with the predicted numerical solution of 0.0180 inches. The small difference is due to the geometric nonlinearity which is included in the finite element solution and ignored in the linear classical solution.

The fuel trays are connected at each corner using compression-only analog elements. A force-deflection curve is applied to each of these elements with a stiffness value representing the respective support (Figure 2). Since there is an initial clearance of 0.11 inches between the trays at the locating pins, an equivalent initial gap (U_0) is included in the force-deflection curve at these locations. The interface forces F_n between the two trays are described as a function of the relative displacements U_n and the clearance U_0 between the two fuel trays. The contact stiffness value K_n applies only when the analog elements are in compression, thus allowing for separation of the trays. The weight of each fuel bundle is applied as nodal loads distributed along the two L-beams at twelve equally spaced locations. The weight of corner supports and locating pin assemblies are applied at the corner nodes. The section property definitions account for the weight of the structural beams.

FUEL BUNDLE MODEL

CANDU fuel bundles consist of 37 Zircaloy-4 pencils which have diameters of approximately 13 mm and lengths of 495 mm (Figures 3). The pencils, which are filled with UO_2 pellets, are bundled in an array of 3 concentric rings surrounding one tube at the centre. The Zircaloy-4 end plates, which hold the bundle together, are connected to the pencil end caps using pressure resistant welds. Bearing pads, which support the bundles in the pressure tubes of the nuclear reactor, are located along the outer pencils. The mass of a fuel bundle is 22 kg. The finite element model consists of 6337 nodes, 3462 nonlinear 4-noded shell elements for the end plates, 2072 nonlinear beam elements for the pencils and 78 compression-only analog elements simulating tube contact at the centre of the bundle (Figure 4). A force-deflection curve is applied to each analog element, simulating the contact stiffness when the element is in compression and allowing for separation of the tubes in the opposite direction. The 1.55 mm thick end plates are modelled using shell elements with 3 sampling points through the thickness. The pencils are modelled using a tube stiffness value of $EI=49.14 \text{ N}\cdot\text{m}^2$ (taken from Nadeau, 1992) based on the stiffness of an irradiated fuel element. An equivalent density, representing the weight of the tubes and UO_2 fuel, is calculated and applied to the pencils.

FUEL TRAY INPUT SPECTRA

Specific vibration input data, appropriate for the type of transporter and local road conditions between the irradiated fuel bays and the storage facility, was not available. However, data was available for the transportation of an irradiated fuel cask on local highways using a transport truck travelling at 80 km/h on very poor roads [Forrest 1985]. Since these conditions are much different than those expected during on-site transportation, the data was modified (using velocity and road condition correlations [Forrest 1985]) to represent a transport truck travelling at 20 km/h on a good conditioned road. Figure 5 shows the effect of vehicle velocity and road conditions on the acceleration. Point (1) represents travel at 80 km/h on a very poor road and point (2) represents travel at 20 km/h on a good road. Equation (1) shows the correlation between points (1) and (2).

$$A_{20}^2 = \frac{A_{80}^2}{(1.37)^2(7.38)^2} \quad (1)$$

where: A_{20}^2 = Acceleration PSD value for 20 km/h on good roads
 A_{80}^2 = Acceleration PSD value for 80 km/h on very poor roads

Since the actual transportation condition is approximately 5 km/h on good roads, the applied acceleration PSD is conservative. Figure 6 shows the available 80 km/h data as well as the reduced 20 km/h data used in the analysis. The data is applied to the corner supports of the bottom fuel tray in the form of an acceleration power spectral density curve.

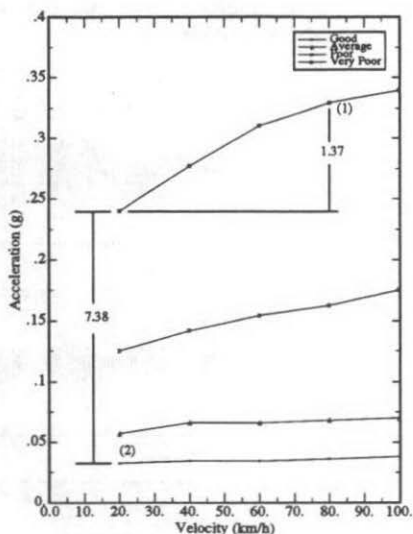


Figure 5: Vertical Acceleration of the Module Stack for Various Road Conditions

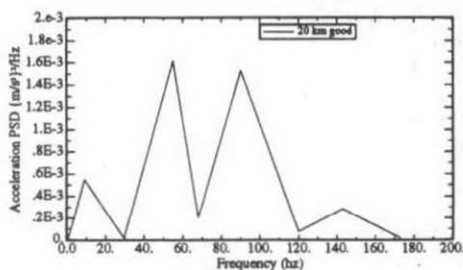
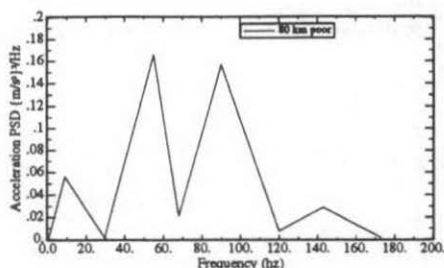


Figure 6: Power Spectral Density Input for Fuel Tray Model

FUEL TRAY VIBRATION

A 10 second simulation was carried out using the nonlinear explicit transient module with the random loading option of the nonlinear finite element code H3DMAP [Sauvé 1995]. For the first 1.5 seconds, only the deadweight loads due to the fuel bundles and trays are applied so that the model attains an equilibrium position. At 1.5 seconds, the vibration input is applied. Relative displacement time histories are shown in Figure 7 for various nodal locations throughout the stack. The relative displacements at the locating pins are not large enough to close the initial gap between the trays. There is a noticeable increase in the relative displacements at locations higher in the stack. This increase is due to the reduced weight on the corner supports at higher locations.

Maximum relative displacements occur at the mid-span of the L-beams. Figure 7 shows the combined displacements of the locating pin and the L-beam deflections. Figure 8 shows the relative mid-span displacement of the L-beams. It is evident from the time histories that the largest deflections occur at node 376, which is located at the mid-span of a locating pin L-beam at the top of the stack. The peak-to-peak maximum relative displacement at this location is small (approximately 0.02 inches).

Figure 9 shows the acceleration time history traces at several locations through the stack. The accelerations are larger along the locating pin L-beams than the corner support L-beams. As well, the accelerations increase at locations higher in the stack. The largest acceleration occurs at the locating pin between the two top trays (node 369) where an rms value of 0.44 g occurs. The results show that

the trays do not separate since the acceleration is less than 1 g at the corner supports. The largest mid-span rms value is approximately 0.27 g and occurs at the top tray (node 793).

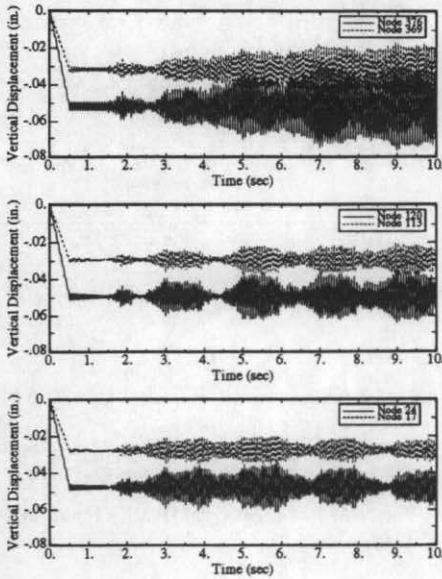


Figure 7: Displacement History for 20 km/h Travel on Good Roads

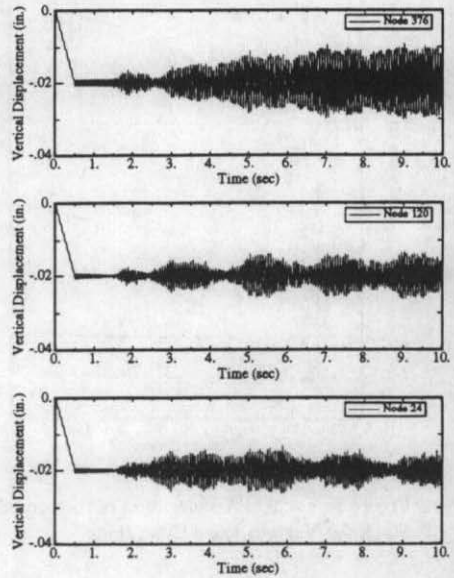


Figure 8: Relative Mid-Span Displacement History for 20 km/h Travel on Good Roads

Figure 10 shows the stress-time history traces at the bottom, middle and top of the stack. Each trace represents the bending stress at the mid-span of a locating pin L-beam where the largest relative displacements occur. As with the displacement and acceleration traces, the stresses increase at higher elevations in the stack. A maximum alternating stress of 10.4 MPa occurs at the mid-span of the top tray (element 367). This is much lower than the endurance limit for 304L stainless steel which is approximately 200 MPa.

FUEL BUNDLE VIBRATION

The maximum acceleration time history is judged to occur at node 369, as shown in Figure 9. This acceleration history is used as input for the fuel bundle vibration analysis. Since there appear to be repeatable time-history blocks of acceleration, a two second period is used for input for the analyses. The acceleration input is applied to the fuel bundle through the mass degrees of freedom at the three bearing pads.

Figure 11 shows the two locations on the end plate with the highest stresses resulting from the vibration analysis. The area on the outer ring (element 2658) is located near a fuel pencil attachment. The high stresses in this area are due to the fact that the input vibration is applied to the adjacent pencil. There are also high stresses at one of the cross braces (element 5420). This element is in a high stress concentration region where the cross brace joins with the centre ring. The time history for the predicted stress components are shown in Figures 12 and 13 for elements 2658 and 5420.

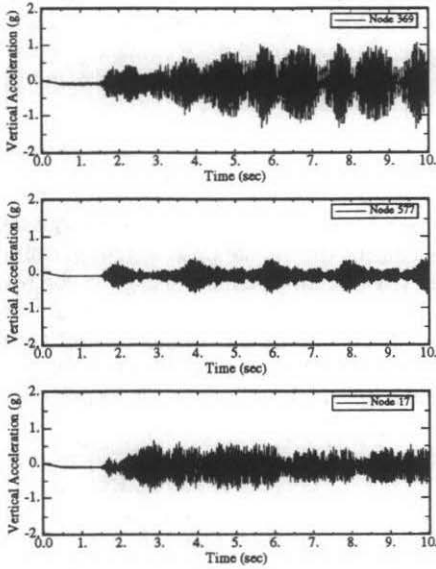


Figure 9: Acceleration History for 20 km/h Travel on Good Roads

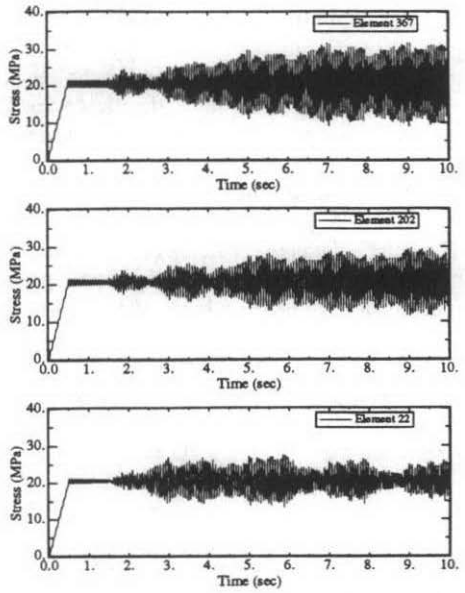


Figure 10: Stress History for 20 km/h Travel on Good Roads

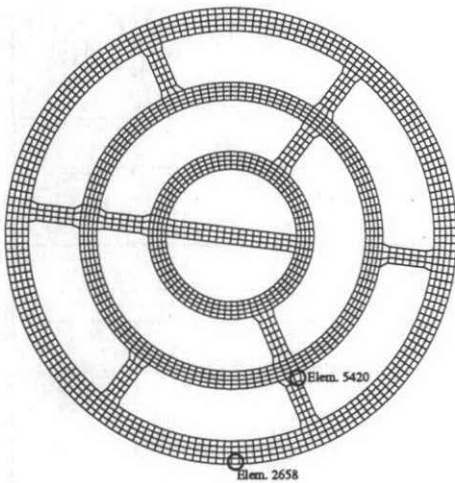


Figure 11: Locations of Maximum End Plate Stress

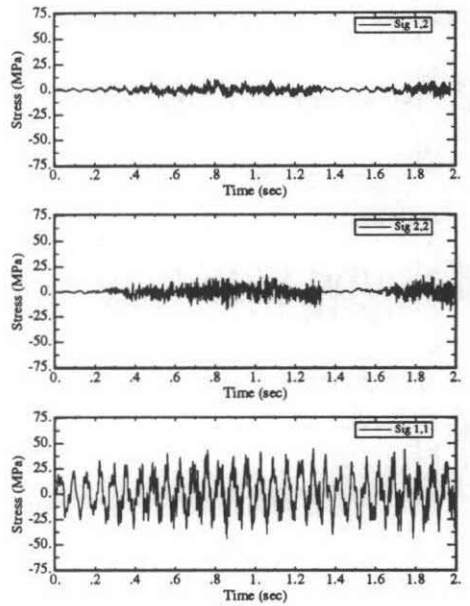


Figure 12: Stress Component History for Shell Element 2658

Stresses along the Zircaloy-4 pencils are low compared to the end plate stresses. The more flexible tubes transmit most of their energy to the stiffer end plates. Although the stresses are lower, the weld interfaces between the tubes and end plate are investigated for possible fatigue damage. Figure 14 shows the stress component time histories for element 225, which is located at the tube/end plate interface on a pencil subjected to input vibration.

FUEL BUNDLE DAMAGE CALCULATION

The fatigue damage is calculated for elements 2658, 5420 and 225, during the vibration analyses, and prorated to account for the longer time period expected during the on-site transportation. Damage is calculated using a combination of a multiaxial fatigue cycle counting method (using the von Mises equivalent stress) [Byrne 1997], a Goodman diagram (to account for the mean stress), a best-fit damage curve for irradiated Zr-2, Zr-3 and Zr-4 at 600 deg. F. [O'Donnell-Langer 1964] and the Miner Rule. The damage calculation for element 225 in the end cap/end plate weld was based on the lower bound of fatigue test results for end plate to end cap welds [Ho et. al. 1991], where the nominal stresses in the fuel pencil are plotted against cycles to failure.

Although the finite element model accounts for some of the stress concentration effects, a fatigue notch factor of 4 was applied to the stresses for the fatigue analysis of elements 2658 and 5420. Assuming a 2 hour travel period, the predicted fatigue usage factor is 4% for element 2658 and 18% for element 5420. Damage in element 225 is calculated by applying a safety factor of 2 to all of the stress components. The predicted damage is negligible since the calculated maximum stress range is less than the nominal stress endurance limit.

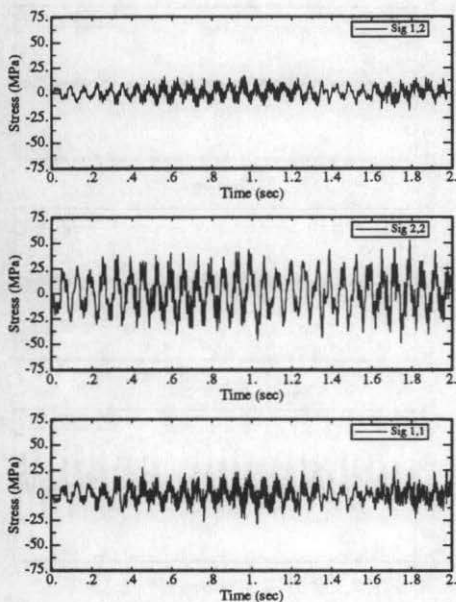


Figure 13: Stress Component History for Shell Element 5420

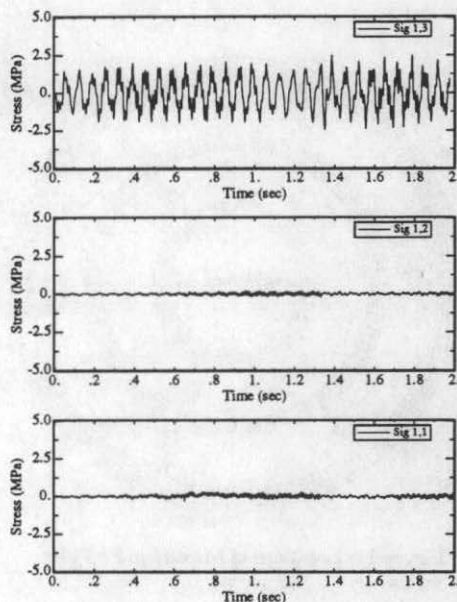


Figure 14: Stress Component History for Beam Element 225

CONCLUSIONS

A stack of 25 irradiated-fuel bundle trays is subjected to the vibration spectra from a transport truck travelling at 20 km/h on a road of good condition. The relative displacements and rms accelerations are small and there is no evidence of the trays separating. The maximum alternating normal stresses are much lower than the endurance limit for the tray material. Since the applied transportation conditions are conservative when compared to the expected conditions of 5 km/h on good-conditioned roads, the analysis demonstrates that the fuel tray support structure meets the requirements for the on-site transportation of irradiated fuel bundles.

The maximum predicted accelerations, within the trays, were used as input for the vibration and fatigue damage analysis of the irradiated fuel bundles. The resulting stresses in the end cap/end plate weld are lower than the endurance limit. However, a usage factor of 18% was calculated based on the maximum damage to the fuel bundle end plate during a 2 hour travel period. This calculation is based on the application of a fatigue notch factor of 4 to the predicted stress components (which also contain a nominal stress amplification due to the finite element modelling).

ACKNOWLEDGMENT

The authors would like to thank Dr. Richard Sauvé for his valuable advice and support.

REFERENCES

- Beer, F.P., Johnston, E.,R., *Mechanics of Materials*, McGraw-Hill, 1981.
- Forrest, J.W., *Irradiated Fuel Transportation Shock and Vibration Program - Phase II Summary*, OHRD Report No. 85-190-K, August, 1985.
- Nadeau, E., *Dynamic Simulation of Darlington NGS Fuel*, OHRD Report No. 92-53-k, March 27, 1992.
- Sauvé, R.G., *H3DMAP Version 6 - A General Three-Dimensional Finite Element Computer Code for Linear and Nonlinear Analysis of Structures*, OHT Report No. A-NSG-95-139-P, 1995.
- Byrne, T.P., *A Cycle Counting Technique for Multiaxial Fatigue*, OHT Report No. 5816-002-1997-RA-001-R00, October, 1997.
- O'Donnell, W.J., Langer, B.F., *Nuclear Science and Engineering*, 20.1, 1964.
- Ho, E.T.C., Shek, G.K., Vanderglas, M.L. and Leger, M., *Fatigue Testing of End Plate to End Cap Welds in Support of the Darlington N12 Event Interim Report*, OHT Report No. 91-124-H, July 4, 1991.